Journal of Microscopy, Vol. 235, Pt 1 2009, pp. 1–8
Received 3 August 2008; accepted 9 March 2009

High-aperture cryogenic light microscopy

M.A. LE GROS*,‡, G. McDERMOTT†,‡, M. UCHIDA†,‡,
C.G. KNOECHEL*,‡ & C.A. LARABELL*,†,‡
**Physical Biosciences Division, Lawrence Berkeley National Laboratory, Berkeley, California, U.S.A.*
†Department of Anatomy, University of California San Francisco, San Francisco, California, U.S.A.
‡National Center for X-ray Tomography, Advanced Light Source, Berkeley, California, U.S.A.

Key words. Cellular structures, cryogenic immersion microscopy, fluorescence imaging, protein localization, X-ray tomography.

Summary

We report here the development of instruments and protocols for carrying out high numerical aperture immersion light microscopy on cryogenic specimens. Imaging by this modality greatly increases the lifetimes of fluorescence probes, including those commonly used for protein localization studies, while retaining the ability to image the specimen with high fidelity and spatial resolution. The novel use of a cryogenic immersion fluid also minimizes the refractive index mismatch between the sample and lens, leading to a more efficient coupling of the light from the sample to the image forming system. This enhancement is applicable to both fluorescence and transmitted light microscopy techniques. The design concepts used for the cryogenic microscope can be applied to virtually any existing light-based microscopy technique. This prospect is particularly exciting in the context of 'super-resolution' techniques, where enhanced fluorescence lifetime probes are especially useful. Thus, using this new modality it is now possible to observe dynamic events in a live cell, and then rapidly vitrify the specimen at a specific time point prior to carrying out high-resolution imaging. The techniques described can be used in conjunction with other imaging modalities in correlated studies. We have also developed instrumentation to perform cryo-light imaging together with soft X-ray tomography on the same cryo-fixed specimen as a means of carrying out high content, quantifiable correlated imaging analyses. These methods are equally applicable to correlated light and electron microscopy of frozen biological objects.

Introduction

Light microscopy is one of the most commonplace and informative techniques used in the biological sciences. Over the years, an enormous range of light microscopy methods have been developed, particularly for imaging fluorescence as a means of determining the organization of tagged molecules inside a cell. Fluorescent localization tags can be created in a number of different ways (Giepmans *et al.*, 2006). The most commonly used fluorescent tags are genetically encoded fluorescent protein molecules, or small fluorescent molecules conjugated to antibodies that bind to an epitope on the protein of interest (Giepmans *et al.*, 2006). In practice, virtually any known protein in a cell can now be fluorescently tagged and localized (Shaner *et al.*, 2007). Fluorescent tags are now available in a wide range of colours. Consequently, a number of different proteins can be localized in the same imaging experiment by choosing tags with non-overlapping spectral properties (Shaner *et al.*, 2005). Ideally, the cellular position of these fluorescent tags should be determined with the highest possible spatial resolution (Willig *et al.*, 2006). For many years, the spatial resolution was thought to be limited by diffraction, leading to a maximum resolution limit of typically half the wavelength of the light used (Abbe, 1873), in other words 200 to 300 nm. However, in recent years, a number of 'super-resolution' imaging techniques have been developed that extend beyond this resolution (Hell *et al.*, 2004; Betzig *et al.*, 2006; Rust *et al.*, 2006; Bates *et al.*, 2007; Friedenberger *et al.*, 2007; Willig *et al.*, 2007; Manley *et al.*, 2008; Punge *et al.*, 2008; Schermelleh *et al.*, 2008). All of these methods can be used to localize fluorescent tags in a specimen at a spatial resolution greater than the optical diffraction limit. In all such studies, the fluorescent lifetime of the tag is of paramount importance. Collection of images with consistent fluorescence intensities allows better signal-to-noise measurements, and therefore more accurate localization of the fluorescent signal. Typical estimates of the photon-detection efficiency in a microscope are only around 1%, with a fluorophore typically yielding between 10^5 and 10^6 photons before photo-bleaching occurs (Moerner and Orrit, 1999; Thompson *et al.*, 2002). Allowing for inefficiencies in detection, and other factors, Thompson and colleagues calculated this number of photons

Correspondence to: C.A. Larabell. Tel: 510-486-5890; fax: 510-486-4069; e-mail: Carolyn.Larabell@ucsf.edu

theoretically allows collection of 100 images with a signal sufficient to be localized with a precision of 65 nm, or only 10 images with precision of 20 nm (Thompson *et al.*, 2002) before photobleaching occurs. Consequently, super-resolution methods would benefit greatly from extending the photoactive lifetime of a fluorophore. In general, all fluorescence microscopy experiments are optimal when the fluorophores output a consistent signal over the duration of the experiment. In this paper, we describe the development of a novel cryogenic immersion microscopy method that meets these criteria. The method was designed initially for use in correlated light and soft X-ray microscopy studies (Le Gros *et al.*, 2005; Parkinson *et al.*, 2008), however the methods and instruments used for this purpose are conceptually simple, and therefore have enormous potential to be used in almost any imaging application that could benefit from increased fluorescent probe lifetimes and the use of high numerical aperture (NA) optics. It is well known that cryo-cooling the specimen significantly enhances the lifetime of a fluorophore (Moerner and Orrit, 1999). In our experiments, we have observed a factor of 30 or more increase in the fluorescent lifetime of Yellow Fluorescence Protein (YFP). Moreover, cryogenic microscopy eliminates the need for chemical fixation prior to high spatial resolution imaging. Taken together, these characteristics make high-aperture cryogenic immersion microscopy a new imaging tool with great potential for use as an independent technique, or for producing data on the location of molecules in cells that are also imaged by other modalities (e.g. in conjunction with cryo-electron microscopy studies such as those carried out recently on neurons by Lucic and others (2007), or in the work reviewed in Jensen and Briegel (2007)).

Materials and methods

We took a number of considerations into account when we were designing the prototype high-aperture cryogenic microscope, the most important of which was ensuring the instrument was thermally stable in operation. As with any imaging instrument, a lack of thermal stability can lead to specimen drift during data collection, resulting in blurred images. Obviously, given the large thermal difference between the cryogen and ambient temperature there is more possibility of drift occurring in cryogenic imaging systems. Our other major design considerations were designing an optical system that performed robustly at cryogenic temperatures, and ensuring the immersion fluid was well matched to the refractive index of the cryogenic specimen and the optical system. In this section, we will describe the overall design and use of the microscope.

The overall design of the cryogenic microscope is shown in a CAD model of the instrument in Fig. 1(A) and in greater detail in schematic form in Fig. 1(B) and (C), with details of the specimen imaging compartment and the configuration

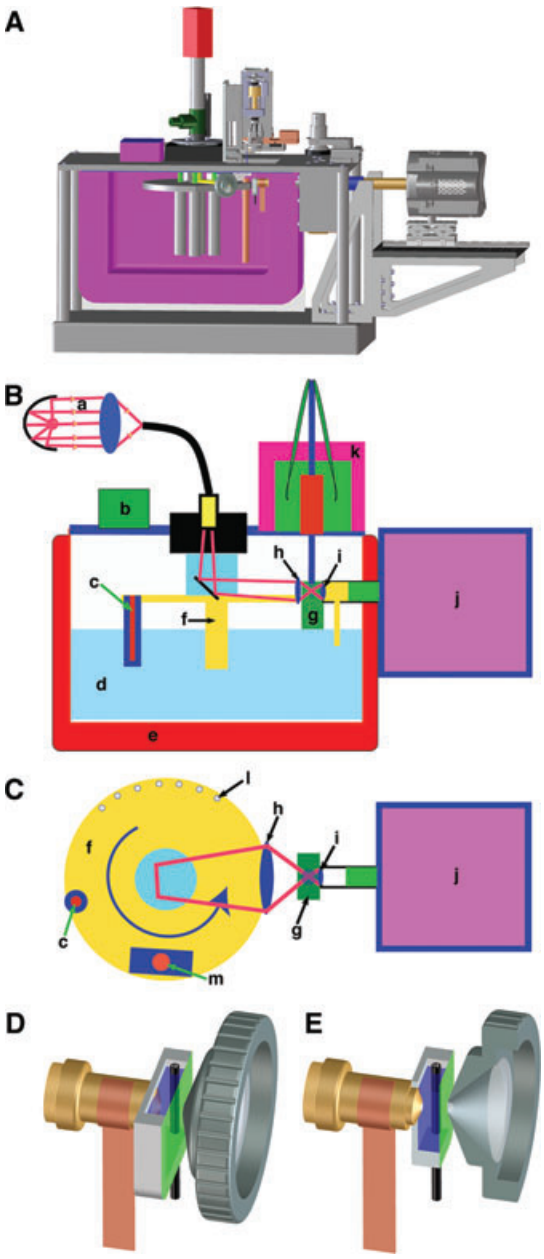

Fig. 1. Schematic of cryogenic immersion light microscope. (A) CAD model of the instrument used for data collection. (B, C) Schematic of the microscope illustrating the light-path and details of the specimen handling instrumentation, viewed from the side (B) and top (C): (a) illumination for bright field imaging; (b) exit port for cryo-transfer; (c) reservoir for propane plunge freezer; (d) liquid nitrogen Dewar; (e) polystyrene insulation for nitrogen Dewar; (f) rotating cryo-platform with conduction cooling rods immersed in liquid nitrogen; (g) liquid propane immersion fluid container; (h) condenser lens; (i) low-temperature, high-aperture objective; (j) CCD detector; (k) dual-purpose sample stage/propane plunge freezer; (l) sample cryogenic storage position; (m) cryo-transfer device. (D) CAD image showing objective (left-hand side) with copper cooling strip, the specimen imaging compartment and the condenser lens. (E) Cut-away of (D) to show details of the specimen imaging compartment. In operation, this contains the cryogenic immersion fluid.

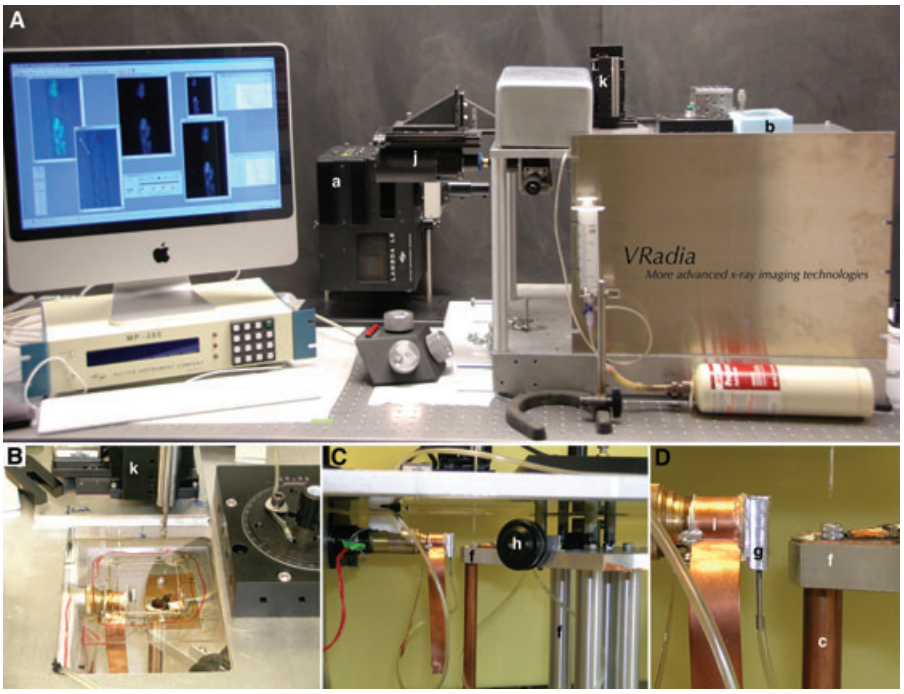

Fig. 2. Photographs of cryogenic immersion light microscope. (A) Photograph of the prototype cryo-microscope in operation. (B) Top view of the specimen imaging compartment and specimen rotation instrumentation. (C) Partially disassembled microscope, showing details of the sample access port with the rotating platform positioned for use of the propane plunge freezer. (D) Close-up of the low-temperature objective and cryogenic immersion fluid container (shown schematically in 1C and 1D) with glass capillary positioned above the container. Those components identified in Fig. 1 that can be readily seen in Fig. 2 are labelled using the same letters for ease of comparison: (a) illumination for bright field imaging; (b) exit port for cryo-transfer; (c) reservoir for propane plunge freezer; (f) rotating cryo-platform with conduction cooling rods immersed in liquid nitrogen; (g) liquid propane immersion fluid container; (h) condenser lens; (j) CCD detector; (k) dual-purpose sample stage/propane plunge freezer.

of the major optical components in Fig. 1(D) and (E). The actual instrument is shown in photographic form in Fig. 2(A–D). As can be seen from these images, our initial 'proof of concept' prototype cryogenic microscope was built from relatively simple, readily available materials and components. To the point, it may appear that minimizing construction costs was a primary consideration. However, this was not the case. The materials used in the construction of the prototype were judiciously chosen based on their thermal properties and their performance in the assembled instrument. This fact, together with iteratively fine tuning the design, resulted in a prototype microscope that was thermally stable and capable of imaging reliably over extended periods of time. In operation, the entire microscope is cooled *en bloc*. Liquid nitrogen is introduced through a porthole and the microscope cooled by filling the reservoir to the appropriate level. There is no need to incrementally cool the system, or any of the optical or mechanical components. The liquid nitrogen reservoir is constructed from a 36 cm × 50 cm × 36 cm polystyrene box. The top plate of the instrument is constructed from a 1.3-cm thick aluminium plate. This forms the attachment surface for all components requiring a high degree of positional stability (e.g. the low-temperature objective lens and the specimen stage). The rotating platform is attached to a rotation stage by four 5-cm diameter fibreglass tubes. The platform is cooled by four 2.5-cm diameter aluminium rods (Fig. 1(B-f)), which extend down into the liquid nitrogen bath (Fig. 1(B-d)). This plate is maintained at a constant temperature of 90 K as long as the liquid nitrogen bath is in contact with the rods. The entire instrument was designed and built in-house by staff of the National Center for X-ray Tomography. The microscope and data collection are both controlled by Image-Pro (Media Cybernetics Inc., Bethesda, MD). Once cold, the microscope can be operated for an entire day with no frosting or drift. The specimen imaging compartment (Fig. 1(D) and (E)) is filled with immersion liquid, typically liquid propane generated by pumping gaseous propane from a standard laboratory cylinder into the imaging compartment using a 50-mL syringe. The design allows the propane level to be topped off if necessary between images. In typical operation, the propane cell is filled every hour. The temperature of the specimen imaging compartment is maintained by conduction through copper strips immersed in the liquid nitrogen reservoir (Fig. 1(D) and (E)). The temperature of the entire microscope remains constant since great care was taken to minimize hot/cold spots, as these could lead to the production of unstable

thermal gradients. The objective lens forms one side of the imaging compartment, with glass forming the other three sidewalls (see Fig. 1(D) and (E)). The objective lens used in the microscope is a standard, readily available optic that has been minimally modified. In our experience, objective lenses are much more robust towards being immersed in cryogen than one might expect. We have repeatedly kept lenses at cryogenic temperatures for extended periods (8–10 h) with no apparent ill effects. We have also subjected the entire optical system to a number of cycles of alternating between room temperature and cryogenic operation. Again, this had no deleterious effects on the microscope, or the optical system. The cryo light microscope can be configured with or without a tube lens. This allows the magnification to be adjusted by either moving the camera or adjusting the tube lens layout, thus allowing for optimization of objective performance. The condenser system is relatively simple, however it is still possible to obtain a condenser with an NA >1. With minor modification, a cryogenic immersion fluid could be used to increase the condenser aperture. Such a system is being developed for implementation of 4 pi light collection and imaging geometries. Multiple cameras can also be used. For example, we have found Qimaging Monochrome Retiga EXi model RET-EXi-F-M-12-C 1392 × 1040 pixel (Qimaging, Surrey, BC) fitted with a Sony CCD and a low light EMCCD from ANDOR Inc. (Belfast, Northern Ireland) with a back thinned E2V 500 × 500 cooled CCD model number I-XON 897 to work very well in this instrument. The excitation source can be either a multi-line AOTF modulated Laser source (633 nm, 543 nm, 488 nm and 457 nm) or a broadband Xenon Radio Frequency Plasma Source (Sutter Instruments (Novato, CA) model LAMBDA LS-XL). The instrument is sufficiently stable that it is possible to collect images with exposures as long as 7 s at ~250 nm resolution.

Specimens are either flash frozen by rapidly plunging them into a second cell of cryogen, or cryo-transferred into the robotic specimen handling device (Figs 1(B), 1(C), 2(B) and 2(C)). Specimens are prepared for imaging by mounting them on standard electron microscopy grids, cover slips, or placing them in thin walled glass capillaries. The latter mounting system has been used most frequently since this instrument was primarily designed for correlated light and soft X-ray microscopy studies (e.g. see Parkinson *et al.*, 2008). This specimen mount can be transferred between these two imaging modalities with ease. Capillaries are particularly suited to imaging 'smaller' cells, such as bacteria or yeast. The capillaries used for this purpose range in diameter from 3 to 15 microns. Even at the larger end of this size scale, the thermal conductivity is still sufficiently rapid that the specimen cools without the formation of potentially damaging ice crystals. Since the capillaries have a wall thickness ~150 nm, there is no significant aberration due to the difference in refractive index of the glass and the cryogenic immersion fluid.

Our prototype high-aperture cryogenic microscope design is shown in Fig. 1(A–E), and photographs of the functional microscope in Fig. 2(A–E). The microscope was designed to allow specimens in a variety of mounts to be flash frozen and immediately imaged, or frozen and stored in the instrument for imaging at a later date (the design of this automated cryogenic specimen handling device is shown in Fig. 1(C)). Having the opportunity to freeze and store a number of specimens at specific points in time also makes this technique well suited to time-dependent imaging studies. The prototype high-aperture cryogenic microscope was designed to operate in conjunction with a soft X-ray microscope (XM-2) at the National Center for X-ray Tomography (see http://ncxt.lbl.gov for further details). The new instrument was designed to function as a platform for specimen vitrification, short-term cryo-storage, correlated light imaging and cryo-transfer to the X-ray microscope for imaging. We have now designed, built and are in the processes of commissioning the next generation cryogenic microscope. The design of this new instrument incorporates a number of improvements that are based on our experience imaging cells using the prototype microscope.

To facilitate our description of how the high-aperture cryogenic microscope is used, we will refer to the simple schematic of the microscope components in Fig. 1(B) and (C). Specimens are manipulated using a 3-axis stepper motor stage located on top of the cryogenic microscope (Fig. 1(B-k)). This stage also contains a spring-driven plunge freezer that is used to rapidly vitrify specimens in a propane reservoir (Fig. 1(B-c)). Following vitrification, the specimen is moved from the liquid propane freezing reservoir into the liquid nitrogen temperature dry atmosphere of the cryo-microscope and then translated to the liquid propane imaging reservoir (Fig. 1(B-g)). Propane is a suitable low-temperature fluid with a high refractive index (1.33), and is therefore well matched to the 1.3 NA lens used in the microscope. The objective lens used for the current measurements is a modified hybrid constructed from a Fratelli Koristka lens 30× NA 1.00 and a Spencer Lens Company (Germany) 82× NA 1.33 oil lens. Finally, the rotating cryo-platform (Fig. 1(B-f)) is positioned to move the cryogenic condenser lens (Fig. 1(B-h)) opposite to the high-aperture objective (Fig. 1(B-i)). The bright field illumination is provided by a halogen lamp (Fig. 1(B-a)) coupled to the cryo-storage unit by a fibre light guide aimed at a plane mirror aligned with the condenser lens, both of which rotate with the cryo-platform. Bright field light microscopy is first used to locate samples of interest. In the first instance, the CCD detector (Fig. 1(B-j)) is moved closer to the objective (Fig. 1(B-i)). This increases the field of view and reduces the magnification. Once a specimen of interest is found, the detector is moved back to a position that produces the desired field of view and magnification. High-aperture multi-wavelength fluorescence microscopy can then be performed on the sample by moving the appropriate dichroic filter into position and switching the illumination source. Illumination

for fluorescence measurements is provided by a liquid light guide coupled xenon light source. The microscope is outfitted with a sliding holder containing three positions for dichroic filter cubes. These are manually positioned to select the desired excitation dichroic and emission filters (for clarity, the filter block assembly is not shown in the schematic; it is located immediately in front of the objective (Fig. 1(B-i)). Once an adequate fluorescence image has been obtained, the specimen can be transferred to a storage position in the robotic specimen handling instrumentation (shown in Fig. 1(C-l)), to await further imaging in the cryogenic microscope or be cryo-transferred to the soft X-ray microscope. The system allows for vitrification, imaging and storage of up to 15 samples. The unit is thermally efficient, and only requires refilling with liquid nitrogen every 6 h. If long-term storage is required, the samples can be cryo-transferred into a long-term liquid nitrogen Dewar. Although this instrument is designed as a stand-alone microscope, it would be possible with minimal redesign effort to adapt it for a standard commercial microscope. We recently coupled it with our Zeiss LSM 510 NLO imaging system.

Specimen preparation for cryogenic microscopy

E. coli bacteria were transformed with a pET-23b vector containing a C-terminal His-Tag sequence (EMD Chemicals, Inc., Gibbstown, NJ) containing six histidines plus the coding sequence for yellow fluorescent protein. Cells were grown to mid-log phase in LB medium and expression of the plasmid induced by adding IPTG to a final concentration of 1 mM. After 2 h, the resultant over-expression of YFP caused the cells to appear yellowish green. The expressed YFP construct has no bacterial function, and was distributed throughout the cell, with the exception of a single region that is likely an inclusion body, comprised of mis-folded protein molecules. Since yellow fluorescent protein has to fold properly to fluoresce, this explains the lack of YFP emission signal. This explanation also correlates with the high density of this region when cells are imaged using soft X-ray tomography shown in Fig. 3(D) and (E).

Wild-type *S. pombe* cells (strain #972 h) were grown with rotary shaking at 30°C in YES media (yeast extract + adenine + casamino acids) supplemented with leucine, histidine, uracil and dextrose. Vacuoles were stained by the addition of 5-chloromethyl fluorescein diacetate (CMFDA; Molecular Probes®, Invitrogen, Carlsbad, CA) to a final concentration of 2.5 μM in growth media.

NIH/3T3 cells (ATCC) were maintained in DME (ATCC) supplemented with 10% bovine calf serum (ATCC) then plated at a density of 25,000 cells/cm^2 on poly-L-lysine-coated glass cover slips and allowed to attach for 16–24 h. Cells were then fixed with 4% formaldehyde and 0.1% glutaraldehyde (30 min at room temperature) then permeabilized with 0.1% saponin. For actin labelling, cells were incubated in a 1:40 solution of ALEXA-488-conjugated phalloidin (Invitrogen) for 60 min at room temperature.

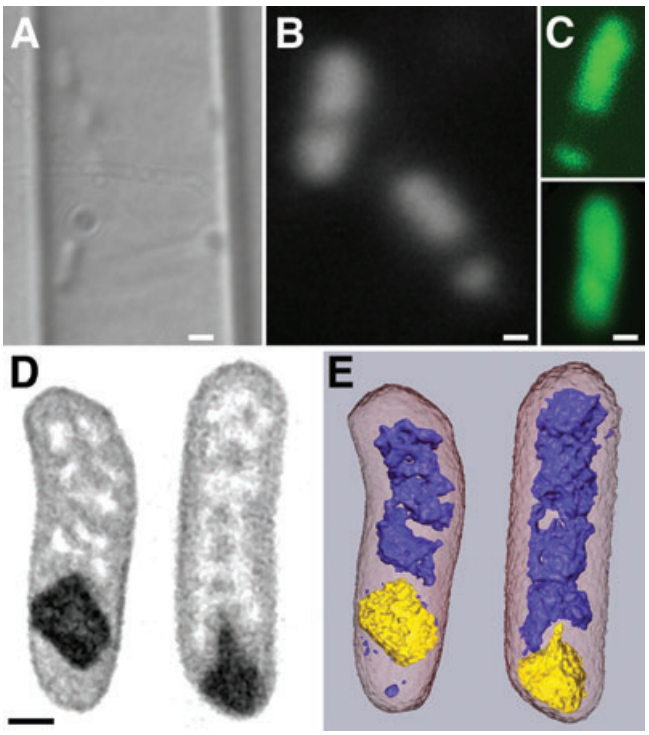

Fig. 3. Correlated light and X-ray images of *E. coli* expressing YFP. (A) Bright field image of *E. coli,* in a glass capillary, taken with cryogenic light microscope; (B) low-temperature, high-aperture fluorescence image of *E. coli*; (C) scanning confocal images of *E. coli*, collected at room temperature; (D, E) soft X-ray tomography of two different *E. coli* seen in single orthoslices from the tomographic reconstruction in (D), where black structures are the least absorbing (least dense) nucleoid, which has been segmented and colour-coded blue in (E), and the white structures are the most absorbing (most dense) inclusion bodies, which have been segmented and colour-coded yellow in (E); data were segmented using the program AMIRA. Scale bars = 1 um (A) and 250 nm (B–E).

Photo-bleaching experiments

The microscope was set up to continuously record fluorescence images of bacteria expressing YFP that had been mounted in a thin-walled capillary. Measurements were collected at room temperature every 50 milliseconds for a total cumulative exposure time of 10 min. The total fluorescence intensity was integrated in each image and plotted against time. The experiment was repeated using a similar specimen and the same data collection parameters, but with the microscope operated at cryogenic temperature.

Soft X-ray tomography of E. coli

Soft X-ray tomography of *E coli* cells was carried out using the instruments and methods described in Le Gros *et al.* (2005).

Results

Using our prototype microscope, we imaged a number of bacterial and yeast cells that contained fluorescent signals. Figure 3 shows *Escherichia coli* cells expressing YFP imaged by high-aperture cryogenic microscopy (Fig. 3(A) and (B)), conventional room temperature confocal microscopy (Fig. 3(C)) and soft X-ray tomography (Fig. 3(D) and (E)). All of these methods show very close correlation in terms of the pattern of fluorescence localization (and with that of earlier work (Miao *et al.*, 2003)). We used similar cells to determine the extent to which the fluorescence lifetime is increased, and compared the time to photo-bleach cells at room temperature and at liquid nitrogen temperature. These data are shown graphically in Fig. 4. As can be seen from these graphs, the half time to fluorescence photo-bleaching of the YFP was extended by a factor of approximately 30. We also observed very similar enhancement of fluorescence lifetime when the specimen was the yeast *Schizosaccharomyces pombe*, which had the vacuoles stained with the small molecule fluorescent label CMFDA (5-chloromethyl fluorescein diacetate; Molecular Probes Inc). Representative images are shown in Fig. 5. This methodology can also be used to obtain high-quality images of fluorescently tagged proteins, such as actin, in cells grown on cover slips, as seen in Fig. 6.

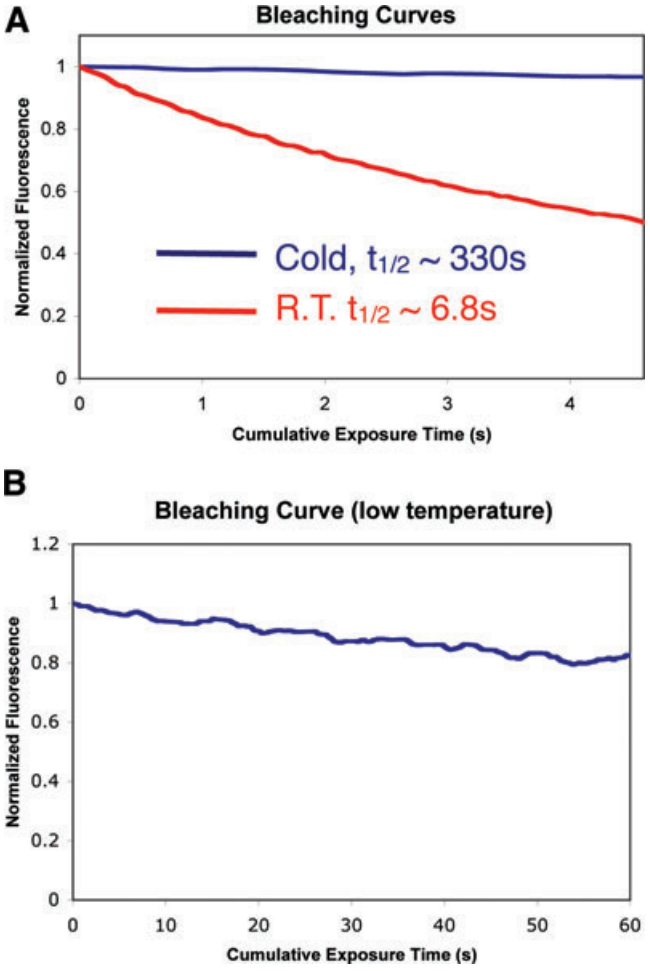

Fig. 4. Photobleaching curves for yellow fluorescent protein, (YFP), expressed in *E. coli*. (A) The blue curve shows fluorescence decay at liquid nitrogen temperature; the red curve shows decay at room temperature. The resistance to photo-bleaching at 77 K is ~50 times that observed at room temperature; (B) low-temperature bleaching curve plotted over a longer time period.

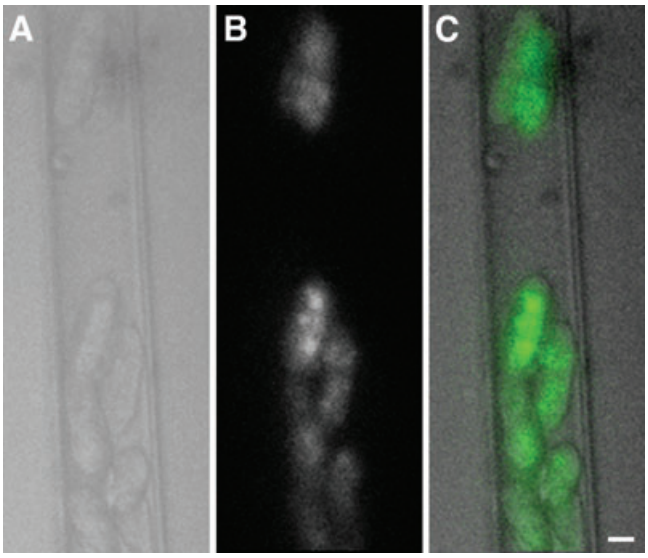

Fig. 5. Cryogenic images of *S. pombe* cells. (A) Brightfield images of *S. pombe* in glass capillary that is approximately 8 um in diameter; (B) fluorescence images of *S. pombe* cells showing vacuoles labelled with the small molecule CMFDA (5-chloromethyl fluorescein diacetate; Molecular Probes Inc), with the cell in the approximate centre of the field of view in best focus; (C) overlay of A and B. Scale bar = 2 um.

Discussion and conclusions

The development of a high-aperture cryogenic immersion microscope meets several long-standing unmet needs in biological and biomedical research. To our knowledge, this is the first report of biological cryogenic imaging that uses high-aperture optics and immersion fluids. As has been established in high-resolution electron microscopy, cryogenic fixation results in specimens that are more closely representative of the native state than that observed in specimens that have been subjected to chemical fixation methods (Dubochet *et al.*, 1988). This alone is sufficient justification for considering adopting cryogenic light-based techniques for experiments where fixation is required. However, an even greater benefit to using cryo-light imaging is the observed increase in fluorophore lifetime. Although low-temperature microscopes have previously been used to view frozen cells, the introduction of a low-temperature immersion lens approach has opened

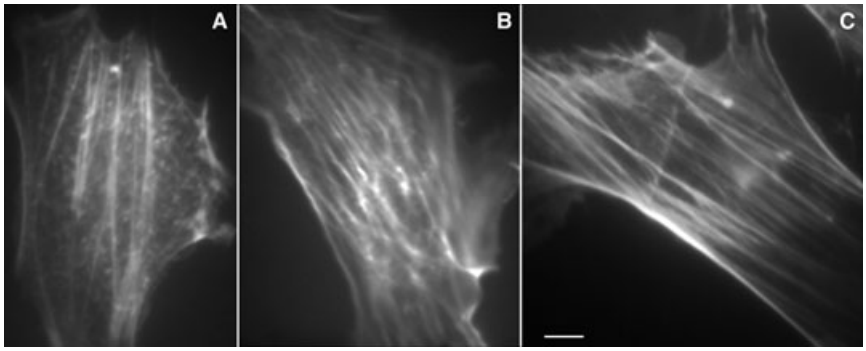

Fig. 6. Cryogenic images of fluorescently labelled actin in NIH 3T3 cells. Cells were grown on glass cover slips and labelled with ALEXA-488-conjugated phalloidin. Scale bar = 1 um.

up the possibility of using the highest resolution fluorescence imaging methods on a vitrified sample prior to X-ray or electron microscopy. In recent years, much time and effort has been spent enhancing genetically encodable molecules, such as Fluorescent Proteins. However, little of this work has been dedicated to specifically increasing the fluorescent lifetime of these molecules (Ai *et al.*, 2006; Shaner *et al.*, 2008). In our experience, cryogenic imaging results in a significant increase in the useful working life of all fluorophores. This characteristic is highly desirable in general, but will be particularly useful in 'super resolution' imaging techniques such as 3-dimensional structured illumination microscopy (Carlton, 2008), or any other method that can benefit from the collection of comparatively large numbers of images. Typically, the highest possible spatial resolution description of the fluorescence signal, and therefore the precision with which relative protein locations can be determined is a trade-off between image collection and photon damage (Schermelleh *et al.*, 2008).

Currently, 'super resolution' fluorescence microscopy methods such as PALM or STORM (Hell *et al.*, 2004; Betzig *et al.*, 2006; Rust *et al.*, 2006; Willig *et al.*, 2006; Bates *et al.*, 2007; Friedenberger *et al.*, 2007; Willig *et al.*, 2007) can be used to determine localization of molecules to better than 10 nm, but only under high NA imaging conditions in thin specimens. High NA imaging requires the use of an index matching immersion fluid. For room temperature microscopy, this fluid is usually oil (refractive index $\sim$1.5) for fixed samples, or water (refractive index 1.33) for live cells. Other more generally applicable super resolution methods such as STED (Punge *et al.*, 2008) and structured illumination microscopy (Carlton, 2008) can be used in whole cells. To attain the maximum resolution possible with these methods, the specimen must be fixed (to avoid movement artefacts) or the region examined must be very thin.

In summary, there are a number of advantages to performing fluorescence imaging at cryogenic temperatures. First, the sample is held in a vitrified state, considered to be the least disruptive fixation method, and therefore does not move during the time required for collection of a 3-D imaging data set. Secondly, fluorescent probes have a greatly enhanced fluorescence lifetime. Thirdly, the spectral width of the emitted light is narrower than at room temperature (Moerner and Orrit, 1999), allowing the use of narrow band emission filters and further increasing the available signal to background. Fourthly, photo-bleaching should be independent of local chemical environment in a frozen sample, which means it is possible to perform a quantitative measurement of local concentration of the labelled protein. By using a custom objective lens that can operate at liquid nitrogen temperature, we have been able to employ refractive index matching fluids, such as liquid propane (refractive index 1.32) or iso-pentane (refractive index 1.35) to perform high-aperture (that is to say an NA greater than 1.3) cryogenic visible light microscopy. This is a significant improvement over those approaches employing dry lenses, which are limited to an NA $<$1 and suffer from image degradation as a result of strongly scattered light traversing the boundary between two media of widely differing refractive indexes, as would occur between a hydrated biological specimen and air or a vacuum. The use of a cryogenic immersion fluid with a refractive index matched to the sample and objective lens greatly reduces such problems allowing fluorescence imaging that is equal, or better than that obtained with high NA lenses using conventional room temperature immersion media.

Acknowledgements

The authors thank Zeny Serrano for culturing cells and assisting with the fluorescence staining, and Dula Parkinson for his assistance in calculating the fluorescent lifetimes. This work was funded by the US Department of Energy, Office of Biological and Environmental Research (DE-AC02–05CH11231), the National Center for Research Resources of the National Institutes of Health (PRR019664) and the National Institutes of General Medical Sciences of the National Institutes of Health (GM63948). MAL and CAL hold patents for the cryogenic immersion

microscope (WO/2006/113916) and the cryo-tomography X-ray microscope stage (WO/2006/113908A2).

References

Abbe, E. (1873) Beiträge zur Theorie des Mikroskops und der mikroskopischen Wahrnehmung. *Arch. Mikrosk. Anat.* **9**, 413–468.

Ai, H.W., Henderson, J.N., Remington, S.J. & Campbell, R.E. (2006) Directed evolution of a monomeric, bright and photostable version of Clavularia cyan fluorescent protein: structural characterization and applications in fluorescence imaging. *Biochem. J.* **400**, 531–540.

Bates, M., Huang, B., Dempsey, G.T. & Zhuang, X. (2007) Multicolor super-resolution imaging with photo-switchable fluorescent probes. *Science* **317**, 1749–1753.

Betzig, E., Patterson, G.H., Sougrat, R., *et al.* (2006) Imaging intracellular fluorescent proteins at nanometer resolution. *Science* **313**, 1642–1645.

Carlton, P.M. (2008) Three-dimensional structured illumination microscopy and its application to chromosome structure. *Chromosome Res.* **16**, 351–365.

Dubochet, J., Adrian, M., Chang, J.J., Homo, J.C., Lepault, J., McDowall, A.W. & Schultz, P. (1988) Cryo-electron microscopy of vitrified specimens. *Q. Rev. Biophys.* **21**, 129–228.

Friedenberger, M., Bode, M., Krusche, A. & Schubert, W. (2007) Fluorescence detection of protein clusters in individual cells and tissue sections by using toponome imaging system: sample preparation and measuring procedures. *Nat. Protoc.* **2**, 2285–2294.

Giepmans, B.N., Adams, S.R., Ellisman, M.H. & Tsien, R.Y. (2006) The fluorescent toolbox for assessing protein location and function. *Science* **312**, 217–224.

Hell, S.W., Dyba, M. & Jakobs, S. (2004) Concepts for nanoscale resolution in fluorescence microscopy. *Curr. Opin. Neurobiol.* **14**, 599–609.

Jensen, G.J. & Briegel, A. (2007) How electron cryotomography is opening a new window onto prokaryotic ultrastructure. *Curr. Opin. Struct. Biol.* **17**, 260–267.

Le Gros, M.A., McDermott, G. & Larabell, C.A. (2005) X-ray tomography of whole cells. *Curr. Opin. Struct. Biol.* **15**, 593–600.

Lucic, V., Kossel, A.H., Yang, T., Bonhoeffer, T., Baumeister, W. & Sartori, A. (2007) Multiscale imaging of neurons grown in culture: from light microscopy to cryo-electron tomography. *J. Struct. Biol.* **160**, 146–156.

Manley, S., Gillette, J.M., Patterson, G.H., Shroff, H., Hess, H.F., Betzig, E. & Lippincott-Schwartz, J. (2008) High-density mapping of single-molecule trajectories with photoactivated localization microscopy. *Nat. Methods* **5**, 155–157

Miao, J., Hodgson, K.O., Ishikawa, T., Larabell, C.A., LeGros, M.A. & Nishino, Y. (2003) Imaging whole *Escherichia coli* bacteria by using single-particle x-ray diffraction. *Proc. Natl. Acad. Sci. USA* **100**, 110–112.

Moerner, W.E. & Orrit, M. (1999) Illuminating single molecules in condensed matter. *Science* **283**, 1670–1676.

Parkinson, D.Y., McDermott, G., Etkin, L.D., Le Gros, M.A. & Larabell, C.A. (2008) Quantitative 3-D imaging of eukaryotic cells using soft X-ray tomography. *J. Struct. Biol.* **162**, 380–386.

Punge, A., Rizzoli, S.O., Jahn, R., Wildanger, J.D., Meyer, L., Schonle, A., Kastrup, L. & Hell, S.W. (2008) 3D reconstruction of high-resolution STED microscope images. *Microsc. Res. Tech.* **71**, 644–650.

Rust, M.J., Bates, M. & Zhuang, X. (2006) Sub-diffraction-limit imaging by stochastic optical reconstruction microscopy (STORM). *Nat. Methods* **3**, 793–795.

Schermelleh, L., Carlton, P.M. Haase, S., *et al.* (2008) Subdiffraction multicolor imaging of the nuclear periphery with 3D structured illumination microscopy. *Science* **320**, 1332–1336.

Shaner, N.C., Steinbach, P.A. & Tsien, R.Y. (2005) A guide to choosing fluorescent proteins. *Nat. Methods* **2**, 905–909.

Shaner, N.C., Patterson, G.H. & Davidson, M.W. (2007) Advances in fluorescent protein technology. *J. Cell Sci.* **120**, 4247–4260.

Shaner, N.C., Lin, M.Z., McKeown, M.R., Steinbach, P.A., Hazelwood, K.L., Davidson, M.W. & Tsien, R.Y. (2008) Improving the photostability of bright monomeric orange and red fluorescent proteins. *Nat. Methods* **5**, 545–551.

Thompson, R.E., Larson, D.R. & Webb, W.W. (2002) Precise nanometer localization analysis for individual fluorescent probes. *Biophys. J.* **82**, 2775–2783.

Willig, K.I., Harke, B., Medda, R. & Hell, S.W. (2007) STED microscopy with continuous wave beams. *Nat. Methods* **4**, 915–918.

Willig, K.I., Kellner, R.R., Medda, R., Hein, B., Jakobs, S. & Hell, S.W. (2006) Nanoscale resolution in GFP-based microscopy. *Nat. Methods* **3**, 721–723.

